

Photobleaching of light-induced paramagnetic defects in fast and slow processes in $a\text{-Si}_{1-x}\text{N}_x\text{:H}$ alloys

Jinyan Zhang, Qing Zhang, Minoru Kumeda, and Tatsuo Shimizu

Faculty of Technology, Kanazawa University, Kanazawa 920, Japan

(Received 8 August 1994)

The photobleaching of light-induced metastable dangling bonds (DB's) in Si-rich $a\text{-Si}_{1-x}\text{N}_x\text{:H}$ alloys is carried out using subgap illumination at both room temperature (RT) and liquid-nitrogen temperature (77 K). The photobleaching is mainly aimed at the light-induced DB's in the two different processes: the fast process and the slow process. Combining the results of photobleaching with those for RT annealing of the light-induced DB's in both processes created at 77 K, we find that there are prominent differences between the natures of light-induced DB's in the two processes: (1) The light-induced DB's in the fast process can be bleached by subgap illumination, while those in the slow process cannot; (2) the light intensity needed for generating the light-induced DB's in the slow process is stronger than that for the light-induced DB's in the fast process. A comparison of the present results with those for $a\text{-Si:H}$ shows that the light-induced DB's in the fast process are similar to the light-induced DB's created by low-intensity light at low temperature in $a\text{-Si:H}$, and the light-induced DB's in the slow process are similar to the light-induced DB's created by high-intensity light at RT in $a\text{-Si:H}$. The results suggest that the light-induced DB's in the fast process are associated with charge trapping and the light-induced DB's in the slow process with the creation of new defects.

I. INTRODUCTION

The investigation of the properties and the creation mechanism of defects in hydrogenated amorphous silicon-nitrogen ($a\text{-Si}_{1-x}\text{N}_x\text{:H}$) alloy films is very important not only for its applications, but also for investigating the relation between the defect creation mechanisms in hydrogenated amorphous silicon ($a\text{-Si:H}$) films and hydrogenated amorphous silicon nitride ($a\text{-Si}_3\text{N}_4\text{:H}$) films. It has been suggested that for the alloy series $a\text{-Si}_{1-x}\text{N}_x\text{:H}$, the defect behavior is distinctly different in Si-rich and N-rich alloys.¹⁻³ Some workers^{2,3} consider that the Si dangling bond (DB) in Si-rich alloys is formed by breaking weak Si-Si bonds, as in the case of $a\text{-Si:H}$, and the Si DB in N-rich alloys is brought about by carrier trapping at preexisting charged defects. The results of a combined measurement of capacitance versus voltage (CV), light-induced electron spin resonance (LESR), and photobleaching of LESR revealed that charge trapping of photoexcited carriers is the main origin of LESR in N-rich alloys.⁴⁻⁷ More recently, however, Kumeda *et al.* reported that two increase processes (called the fast and slow processes) of LESR were observed at both room temperature (RT) and 77 K in Si-rich $a\text{-Si}_{1-x}\text{N}_x\text{H}$ films when they were exposed to strong band-gap light.⁸ It appears difficult to account for the results of the two increase processes of LESR with the model of weak Si-Si bond breaking, which is often used for the interpretation of light-induced defects in $a\text{-Si:H}$.⁹ It was proposed that charge trapping is responsible for the LESR defects in the fast increase process, and breaking of weak Si-Si bonds for the LESR defects in the slow increase process.^{8,10,11} However, there has been no further evidence to verify the proposition.

Photobleaching by sub-gap-light absorption is a signature of charge trapping at preexisting defects in chalcogenide glasses,¹² and in $a\text{-Si:H}$ based alloys,^{6,7,13} because it only influences the distribution of charges in preexisting defects. Therefore, it provides us with a possible way to distinguish between the light-induced neutral DB's produced in the fast and slow processes in Si-rich $a\text{-Si}_{1-x}\text{N}_x\text{:H}$ films, if one of the processes is related to charge trapping.

In this paper, we report the observations of LESR created by high-intensity and low-intensity illuminations, photobleaching of the light-induced spins, and RT annealing behavior of the light-induced spins created at 77 K in Si-rich $a\text{-Si}_{1-x}\text{N}_x\text{H}$ films. In order to make a comparison with $a\text{-Si:H}$, photobleaching of the light-induced spins in $a\text{-Si:H}$ was also done. Our results support the proposition that the LESR signal created by strong band-gap illumination originates from two different sources: charge trapping in preexisting defects and creation of new defects.

II. EXPERIMENT

$a\text{-Si}_{1-x}\text{N}_x\text{:H}$ films used in the investigation were fabricated using the model of glow discharge decomposition. A mixture of undiluted SiH_4 and NH_3 gases was decomposed and the films were deposited on fused-quartz substrates at a temperature of 350°C. The rf power was 0.71 W/cm² and film thicknesses were 2~3 μm. Composition of the films were determined using x-ray photoemission spectroscopy and electron microprobe analysis. The optical gap, determined using the Tauc plot at 300 K, was $E_{\text{opt}}=2.0, 2.2, \text{ and } 2.5$ eV for $x=0.32, 0.40, \text{ and } 0.51$, respectively. The hydrogen content was 29 at. %

for $x=0.40$ and 28 at. % for both $x=0.32$ and 0.51, as determined by IR absorption. High-quality undoped a -Si:H films were deposited on fused-quartz substrates at 300 °C by decomposing SiH_4 in a hot-wall glow-discharge system, which was used to reduce the impurity content in the films.¹⁴ The film thickness was about 3 μm . Before the band-gap illumination, a -Si_{1-x}N_x:H films were annealed at 300 °C for 4 h and a -Si:H films were annealed at 200 °C for 5 h both in flowing nitrogen gas. In the sample with $x=0.32$, the dark spin density of ESR in the annealed state was $N_d=1.2\times 10^{17}\text{ cm}^{-3}$, the g value was $g=2.0044$, the peak-to-peak linewidth of the ESR signal was $\Delta H_{pp}=9.7\text{ G}$; in the sample with $x=0.40$, $N_d=2.7\times 10^{17}\text{ cm}^{-3}$, $g=2.0045$, and $\Delta H_{pp}=10\text{ G}$; and in the sample with $x=0.51$, $N_d=6\times 10^{17}\text{ cm}^{-3}$, $g=2.0042$, and $\Delta H_{pp}=11\text{ G}$.

The ESR measurements were performed in the X band with a JEOL ESR system with a modulation width in the range of 2.5–3.2 G and a microwave power of 0.01 mW at 77 K and 0.1 mW at RT. The microwave powers were ascertained to be low enough to prevent saturation of the signal. The light-induced ESR was observed *in situ* under illumination, except for a -Si:H film. There was no noticeable change in the g value, linewidth, and shape of the ESR signal under or after illumination.

The band-gap illumination for the generation of light-induced defects was done using a high-pressure mercury lamp with a CuSO_4 filter (photon energies of 2.2–4.0 eV) for a -Si_{1-x}N_x:H, providing a maximum intensity of 900 mW/cm², and using a Xe lamp with an IR-cut filter for a -Si:H. The subgap illumination for the photobleaching was done using a Xe lamp with a bandpass filter, the photon energies being 1.10 and 1.46 eV for the samples with $x=0.40$ and 0.51, respectively, and using a tungsten lamp with a bandpass filter with a range of photon energy from 0.60 to 0.99 eV for a -Si:H. To prevent the sample temperature from rising during the band-gap illumination or the subgap illumination at RT, nitrogen gas was flown through the ESR sample tube directly. After cessation of the band-gap illumination, the LESR spin-density decays, and in about 1 h the decay almost stopped. Hence the subgap illumination started 1 h after cessation of the band-gap illumination.

III. RESULTS

A. LESR

The LESR results for strong band-gap illumination for a series of a -Si_{1-x}N_x:H samples ($x=0.32, 0.40,$ and 0.51) show that there are two increase processes, i.e., upon strong band-gap illumination, the ESR spin density increases very rapidly and becomes essentially time independent within 1–2 s (the fast process), and then after a long-time illumination the spin density is observed to increase slowly again (the slow process).^{8,10} A typical example is shown in Fig. 1, where the increment of the ESR spin density is plotted as a function of band-gap illumination time (t_{ill}) for the sample with $x=0.51$ at 77 K and RT. For convenience of description, we define fast DB's (FDB's) as the neutral DB's in the fast process, and slow

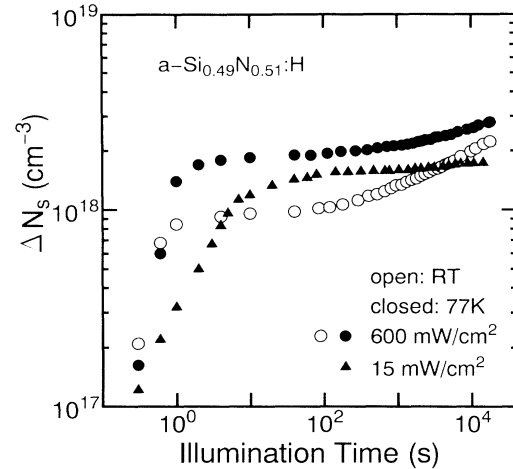


FIG. 1. Increment of the ESR density as a function of band-gap illumination time in the sample with $x=0.51$ at RT (open symbols) and at 77 K (closed symbols). A high-pressure mercury lamp coupled with a CuSO_4 filter is used as the band-gap light source (photon energies of 2.2–4.0 eV). The circles represent $I_B=600\text{ mW/cm}^2$, and the triangles represent $I_B=15\text{ mW/cm}^2$.

DB's (SDB's) as the neutral DB's in the slow process.

To make a comparison between the dependences on light intensity of the creation of FDB's and SDB's, two light intensities, 600 and 15 mW/cm², were used to illuminate the sample with $x=0.51$ at 77 K. It is found from Fig. 1 that the strong band-gap illumination can bring about both increase processes, whereas the low-intensity band-gap illumination seems to produce only the fast process, and upon the low-intensity band-gap illumination the LESR spin density increases more slowly than does the LESR spin density in the fast process created by the high-intensity light. However, these measurements cannot determine whether the increase of LESR created by band-gap illumination is due to the conversion of preexisting charged defects, or due to the creation of new defects.

B. Photobleaching of the light-induced spins

In order to study the creation mechanism of the LESR, we examined the effect of subgap illumination of the light-induced spins at 77 K and RT. For this purpose, we first produced the LESR signals by illuminating the samples with the strong band-gap light either for a short t_{ill} (only FDB's are created) or a long t_{ill} (a mixture of FDB's and SDB's appear), and allowed 1 h to elapse for the decaying, and then subjected the samples to subgap illumination. The illumination time for the production of FDB's was chosen to be short enough to avoid the appearance of SDB's. The g value and linewidth of the photobleached signal were the same as that of the original LESR signal.

Here, we only chose the samples with $x=0.40$ and 0.51 for doing the photobleaching experiment. Figures 2(a) and 2(b) show the change in the ESR spin density

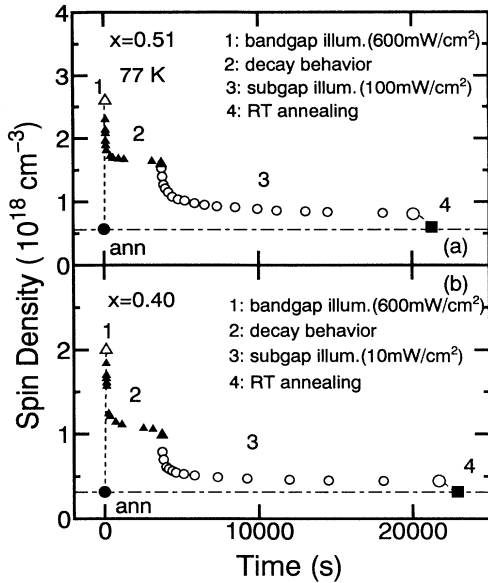


FIG. 2. Change in the ESR spin density at 77 K in the case of a short t_{ill} (100 s): (a) for the sample with $x=0.51$ and (b) for the sample with $x=0.40$. The symbol “ann” indicates annealed states. Symbol “1” represents the treatment of band-gap illumination with $I_B=600$ mW/cm²; “2” the decay after cessation of band-gap illumination; “3” photobleaching by subgap illumination; “4” the treatment of RT annealing for 20 min. The subgap light intensity used for the sample with $x=0.51$ is 100 mW/cm² and for $x=0.40$ is 10 mW/cm².

measured at 77 K in the samples with $x=0.51$ and 0.40, respectively, in four different treatments: (1) band-gap illumination, (2) decay behavior after cessation of the band-gap light, (3) photobleaching by subgap illumination, and (4) RT annealing. Here the intensity of the band-gap illumination is $I_B=600$ mW/cm² and the illumination time is $t_{\text{ill}}=100$ s. The subgap light intensity is $I_s=10$ mW/cm² and 100 mW/cm² for the samples with $x=0.40$ and 0.51, respectively. One sees that after cessation of the band-gap illumination, the ESR spin density decays, and after about 1 h the decay almost stops. It is also noted that after turning on subgap light, the ESR spin density decreases significantly.

Figures 3(a) and 3(b) show the change in the ESR spin density in the samples with $x=0.51$ and 0.40 in the four treatments similar to those mentioned above, where $I_B=600$ mW/cm², $t_{\text{ill}}=5$ h, and the subgap light intensities are the same as in Figs. (a) and 3(b).

We have also done photobleaching of the light-induced spins created by weak band-gap illumination. Figure 4 shows the change in the ESR spin density in the four treatments with $I_B=15$ mW/cm², $t_{\text{ill}}=4$ h, and $I_s=100$ mW/cm². After cessation of the band-gap light, the change in the ESR spin density during the later three treatments resembles the results in Figs. 3(a) and 3(b).

The time dependence of photobleaching at 77 K are replotted on a semilogarithmic scale by closed symbols in Figs. 5(a) and 5(b) for the samples with $x=0.51$ and 0.40,

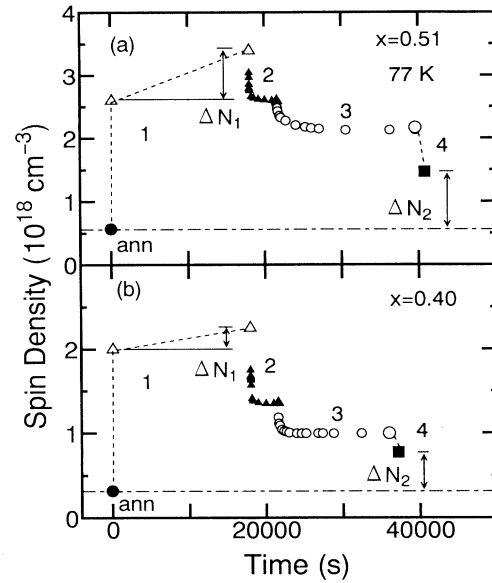


FIG. 3. Change in the ESR spin density at 77 K in the case of a long t_{ill} (5 h): (a) for the sample with $x=0.51$ and (b) for the sample with $x=0.40$. Symbols “1,” “2,” “3,” and “4” have the same meaning as in Fig. 2. For the same sample, the subgap light intensity is the same as in Fig. 2. ΔN_1 indicates the net increase of SDB density, obtained by subtracting the LESR spin density at $t_{\text{ill}}=100$ s from the total LESR spin density created for 5 h. ΔN_2 indicates the remaining fraction of the LESR spin density after RT annealing.

respectively. Photobleaching experiments were also done at RT for the same samples that had been illuminated by strong band-gap light for both a short t_{ill} and a long t_{ill} at RT. For a comparison with the result at 77 K, the data for photobleaching at RT are plotted by open symbols in Fig. 5. The circles are for $t_{\text{ill}}=5$ h and $I_B=600$ mW/cm², the triangles for $t_{\text{ill}}=100$ s and $I_B=600$ mW/cm², and diamonds for $t_{\text{ill}}=4$ h and $I_B=15$ mW/cm². From Figs. 5(a) and 5(b), one finds that the photobleaching of the light-induced spins produced by

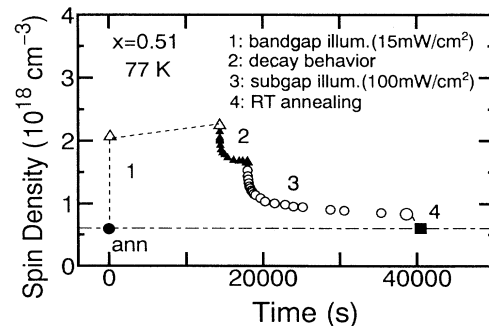


FIG. 4. Change in the ESR spin density at 77 K in the case of $I_B=15$ mW/cm² and $t_{\text{ill}}=4$ h in the sample with $x=0.51$. Symbols “1,” “2,” “3,” and “4” have the same meaning as in Fig. 3.

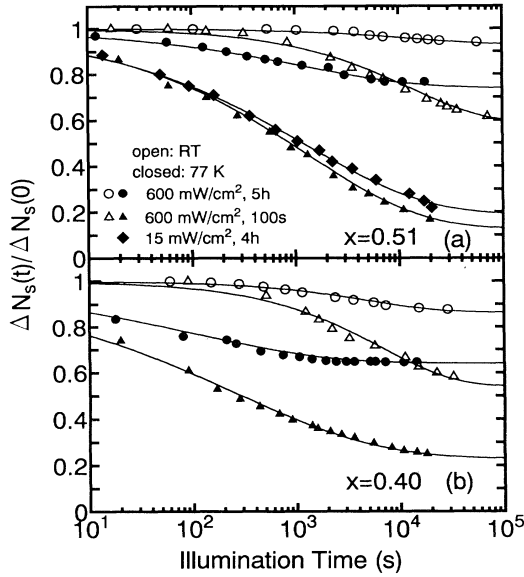


FIG. 5. Photobleaching of LESR as a function of subgap illumination time at RT (open symbols) and 77 K (closed symbols): (a) for the sample with $x = 0.51$ and (b) for the sample with $x = 0.40$. The samples had been illuminated by band-gap light of $I_B = 600 \text{ mW/cm}^2$ for $t_{\text{ill}} = 5 \text{ h}$ (circles), $I_B = 600 \text{ mW/cm}^2$ for $t_{\text{ill}} = 100 \text{ s}$ (triangles), and $I_B = 15 \text{ mW/cm}^2$ for 4 h (diamonds). Solid curves are the fitting lines from Eq. (1).

strong band-gap illumination for a short t_{ill} (100 s), which are considered to be FDB's on the whole, is more prominent than that of the light-induced spins produced by strong band-gap illumination for a long t_{ill} (5 h) at both 77 K and RT. In particular, photobleaching of FDB's at 77 K is more effective. Figures 5 also show that the photobleaching behavior of the light-induced spins produced by weak band-gap illumination (15 mW/cm^2) for 4 h is quite consistent with that for FDB's.

All the photobleaching results in Fig. 5 can be fit with a stretched exponential function

$$\Delta N_s(t)/\Delta N_s(0) = A + [1 - A] \exp[-(t/\tau)^\beta], \quad (1)$$

TABLE I. The best-fitting parameters for Eq. (1) obtained for photobleaching of the LESR in the samples with $x = 0.51$ and 0.40.

x	t_{ill} (s)	I_B (mW/cm ²)	T	$\Delta N_s(0)$ (cm ⁻³)	β	τ (s)
0.51	100	600	RT	4.1×10^{17}	0.60	1.3×10^4
	18000	600	RT	1.7×10^{18}	0.60	1.4×10^4
	100	600	77 K	1.1×10^{18}	0.40	1.3×10^3
	18000	600	77 K	2.0×10^{18}	0.40	1.2×10^3
	14400	15	77 K	1.0×10^{18}	0.40	1.4×10^3
0.40	100	600	RT	1.0×10^{17}	0.62	6.6×10^3
	18000	600	RT	4.1×10^{17}	0.64	5.2×10^3
	100	600	77 K	6.8×10^{17}	0.31	1.0×10^2
	18000	600	77 K	1.0×10^{18}	0.33	2.5×10^2

as shown by the solid curves, where $A = \Delta N_s(\infty)/\Delta N_s(0)$, $\Delta N_s(0)$ is the value of the LESR before bleaching, $\Delta N_s(\infty)$ is the saturated value of the LESR for a long-time subgap illumination, β is a stretched-exponential factor, and τ is a time constant. The parameters for the best fit to the data are listed in Table I. From Table I, one notices that for a given sample at a given temperature, β and τ are essentially independent of t_{ill} . The result suggests that the same kind of DB's are bleached out by subgap light regardless of the band-gap illumination time and intensity, and that the content that have been bleached out are FDB's rather than SDB's.

In order to check the correlation between the nature of the photocreated defects (the Staebler-Wronski effect) in undoped $\alpha\text{-Si:H}$ and FDB's or SDB's in $\alpha\text{-Si}_{1-x}\text{N}_x\text{:H}$ a photobleaching experiment has been carried out in $\alpha\text{-Si:H}$. Before subgap illumination, the undoped sample was illuminated by 3.8 W/cm^2 for 50 h at RT, and the total ESR spin density reached $1.5 \times 10^{17} \text{ cm}^{-3}$. Then it was illuminated by $0.2 \sim 0.3 \text{ W/cm}^2$ subgap light for 487 h at RT. The result showed that after the treatment of subgap illumination there was no appreciable change in the total ESR spin density. Compared with the result in $\alpha\text{-Si:H}$, the nature of SDB is thought to be similar to that of the photocreated DB's in $\alpha\text{-Si:H}$.

C. RT annealing behavior for LESR created at 77 K

After the photobleaching treatments of LESR at 77 K, the samples were kept at RT for about 20 min, and then recooled down to 77 K for detecting ESR signals. From Figs. 2(a) and 2(b), one can see that after RT annealing for 20 min all the FDB's created by a short t_{ill} illumination at 77 K completely recover. On the other hand, for samples illuminated with band-gap light for a long t_{ill} , one can find from Figs. 3(a) and 3(b) that after RT annealing some fraction of the ESR spin density indicated as ΔN_2 in Fig. 3 remains. ΔN_2 is close to, but a little larger than the net increase of the SDB density indicated as ΔN_1 . The results suggests that this fraction of ΔN_2 is mainly created by prolonged high-intensity illumination, which is associated with SDB.

Figure 4 demonstrates that after cessation of the band-

gap illumination, the change in the ESR spin density resembles the results in Fig. 2(a). This result suggests that the LESR created by weak band-gap light for a long t_{ill} is due to FDB's, and that weak band-gap light cannot produce SDB's even though t_{ill} is very long, showing that the band-gap light intensity needed for the production of FDB's is lower than that for the production of SDB's. This set of experimental results implies that FDB's and SDB's are of different origins.

IV. DISCUSSION

In general, the critical composition of $x = 0.52$, corresponding to the percolation threshold of Si-Si bonds in the $a\text{-Si}_{1-x}\text{N}_x\text{:H}$ network, is used for dividing Si-rich and N-rich $a\text{-Si}_{1-x}\text{N}_x\text{:H}$ alloys.³ For $x < 0.52$, both band edges are formed by Si-Si bonding states, and the alloys are regarded as Si rich. Both samples used in the study, with $x = 0.40$ and 0.51 , belong to the group of Si-rich alloys.

Our results show that there are prominent differences between the natures of the FDB and SDB: (i) the FDB can be photobleached, whereas the SDB cannot. (ii) The FDB can be generated even by weak bandgap light, but the SDB can be generated only by stronger band-gap light. (iii) For the same band-gap illumination, the generation rate for FDB's is larger than that for SDB's. It is also interesting to compare these results with the natures of LESR in $a\text{-Si:H}$ and N-rich $a\text{-Si}_{1-x}\text{N}_x\text{:H}$. LESR in $a\text{-Si:H}$ is usually observed at low temperature using low-intensity light, and the fraction of the residual LESR signal, after cessation of the light, becomes larger at lower temperature.¹⁵ The fraction can be photobleached by subgap light with photon energy < 0.7 eV.¹⁶ The light-induced creation of ESR spins at RT, so called the Staebler-Wronski effect (SWE), is another type of light-induced phenomena in $a\text{-Si:H}$. The light-induced spins in this process neither exhibit appreciable decay after cessation of the light, nor suffer from being photobleached as mentioned in the previous section. The comparison shows that the natures of FDB's and SDB's in the present work are very similar to those of LESR at low temperature and the photocreated ESR spins at RT in $a\text{-Si:H}$, respectively.

On the other hand, in N-rich $a\text{-Si}_{1-x}\text{N}_x\text{:H}$, the LESR spin density does not depend much on temperature,² and a large fraction of the LESR spin density remains after cessation of the light, and the residual LESR can be photobleached. The photobleaching behavior of FDB's is essentially the same as that of the light-induced spins in N-rich alloys.⁶ But there are some differences in the aspect of temperature dependence of the stretched exponential parameters, such as β and τ . In our results, the value β at RT is larger than that at 77 K, whereas in N-rich alloys β decrease with increasing temperature from 100 to 298 K. In any case, the result suggests that the nature of FDB's is also similar to the LESR in N-rich alloys.

Now, we consider the creation mechanism of FDB's. Photobleaching of FDB's suggests that the metastability is the result of charge trapping at preexisting charged

DB's, Si_3^- and Si_3^+ during band-gap illumination in analogy with the result for chalcogenide glasses.¹² The reaction can be written as



One has seen that FDB is partially bleached by sub-gap illumination, and the photobleaching effect at 77 K is stronger than at RT as shown in Fig. 5. The fraction of the FDB's that has remained after photobleaching at 77 K completely recover to the annealed states after thermal annealing at RT. Based on these results, we propose the following mechanism for the generation and photobleaching of FDB's: (1) Upon band-gap illumination, charged DB's, Si_3^+ in sp^2 configuration and/or Si_3^- in s^2p^3 configuration convert to neutral DB's Si_3^0 by trapping photoexcited electrons and holes, respectively. (2) The probability for rehybridization from sp^2 or s^2p^3 to sp^3 depends on the illumination intensity and temperature. The higher the illumination intensity or the temperature, the larger the probability.¹¹ Hence, only some fraction of the FDB's are rehybridized to sp^3 configuration. (3) After cessation of the band-gap illumination, the fraction of FDB's that have not been rehybridized recover to the original charged states more easily, leading to the decaying of LESR. (4) The incomplete photobleaching of the FDB's might be directly associated with the structural stability of rehybridized Si_3^0 in sp^3 configuration. During subgap illumination, Si_3^0 in rehybridized sp^3 configuration, which is not too stable, is more easily converted to the original configurations, while Si_3^0 in rehybridized sp^3 configuration, which is stable, is more difficult to be converted to the original configurations.

Next, we discuss the creation mechanism of SDB's. In spite of a large number of investigations on the creation mechanism of the metastable defects in $a\text{-Si:H}$ and its alloys, there has been no experimental or theoretical evidence that has perfectly identified the specific bonding structure related to the SWE. Stutzmann, Jackson, and Tsai proposed that the photocreated defects in $a\text{-Si:H}$ originate from the breaking of weak Si-Si bonds, and the complete microscopic mechanism involves the reconfiguration of Si-H bonds as a stabilizing element.⁹ The model has been widely used for interpretation of the photocreated defects in $a\text{-Si:H}$ and $a\text{-Si:H}$ based alloys. Recent results of pulsed ESR, however, show that the photocreated neutral DB does not have a nearby hydrogen within 4 Å.¹⁷ Hence the stabilizing mechanisms for breaking of weak Si-Si bonds should be improved. The other proposed model for the SWE is charge trapping of photoexcited electrons and holes at charged DB's.¹⁸ If SDB's are also due to charge trapping, the difficulties will appear, i.e., how to imagine a generation mechanism, say charge trapping, which has two different generation rates for light-induced DB's, and how to understand the two different photobleaching behaviors? In accordance with our results, we prefer the creation of new defects, say breaking of weak Si-Si bonds, as the origin of SDB's.

Our results for the Si-rich $a\text{-Si}_{1-x}\text{N}_x\text{:H}$ show that after illumination with 600 mW/cm² for 5 h at RT, the net increase of a SDB, ΔN_1 , is 4.3×10^{16} , 6.2×10^{17} , and

$1.2 \times 10^{18} \text{ cm}^{-3}$ for the samples of $x = 0.32, 0.40,$ and $0.51,$ respectively, indicating that the density of SDB's increase with N concentration. SDB's are thought to be more easily created with increasing N concentration. The possibility that N atoms play a direct role in creating light-induced DB's should be excluded because recent results demonstrate that in $a\text{-Si:H}$ with N impurity the increment in the density of the photocreated spin is one order of magnitude larger than the N concentration.^{17,19} For the interpretation of the effect of incorporation of C, N, and O on the density of photocreated DB's, it was proposed that the impurities lead to an increase of weak bonds in the band tails due to the increased bonding disorder, which could explain the enhanced probability of the metastable DB's.^{20,21} Yokomichi *et al.* suggested that an increase in the structural flexibility due to the incorporation of N, C, and H leads to an increase of the photocreated DB's.²² However, one is still not clear about the microscopic origins of the light-induced SDB's and about the detailed understanding of how these elements, such as, C, N, and O, affect the structure or structural changes in $a\text{-Si:H}$ and $a\text{-Si}$ -based alloys. Further investigations are highly desirable.

V. CONCLUSIONS

Photobleaching of LESR has been observed in Si-rich $a\text{-Si}_{1-x}\text{N}_x\text{:H}$ alloys. The experimental results show that

the behavior of FDB's and SDB's are different: (1) FDB's can be bleached by subgap illumination, while SDB's cannot, (2) the generation of SDB's needs higher light intensity than that of FDB's does, (3) for the same band-gap light intensity, the generation rates for FDB's and SDB's are different, i.e., the rate of creating FDB's is larger than the rate of creating SDB's. The photobleaching behavior of FDB's is similar to that of the light-induced defects in N-rich alloys, and the nature of SDB's is quite similar to that of the photocreated defects in $a\text{-Si:H}$. The metastable LESR created by strong band-gap illumination in Si-rich $a\text{-Si}_{1-x}\text{N}_x\text{:H}$ alloys can be associated with two kinds of origins: the FDB is related to charge trapping among the preexisting charged DB's, Si_3^+ and Si_3^- ; and the SDB is related to the new creation of neutral DB's.

ACKNOWLEDGMENTS

The authors are very grateful to Dr. J-H. Zhou for many helpful discussions. The authors thank Dr. A. Morimoto for discussions and assistance in the experiments. The authors also thank A. Sugimoto for his help in fabricating the films used in the study. This work was partly supported by the New Sunshine Project of the Ministry of International Trade and Industry in Japan.

-
- ¹J. Robertson, *Philos. Mag. B* **63**, 47 (1991).
²W. L. Warren, J. Kanicki, F. C. Rong, W. R. Buchwald, and M. Harmatz, in *Wide Band-Gap Semiconductors*, edited by T. D. Mousatakas, J. I. Pankove, and Y. Hamakawa, MRS Symposia Proceeding No. 242 (Materials Research Society, Pittsburgh, 1992), p. 687.
³J. Robertson, *Philos. Mag. B* **69**, 307 (1994).
⁴S. E. Curry, P. M. Lenahan, D. T. Krick, J. Kanicki, and C. T. Kirk, *Appl. Phys. Lett.* **56**, 1359 (1990).
⁵D. T. Krick, P. M. Lenahan, and J. Kanicki, *Phys. Rev. B* **38**, 8226 (1988).
⁶E. D. Tober, J. Kanicki, and M. S. Crowder, *Appl. Phys. Lett.* **59**, 1723 (1991).
⁷H. Fritzsche and Y. Nakayama, *Philos. Mag. B* **69**, 359 (1994).
⁸M. Kumeda, A. Sugimoto, J. Zhang, Y. Ozawa, and T. Shimizu, *Jpn. J. Appl. Phys.* **32**, L1046 (1993).
⁹M. Stutzmann, W. B. Jackson, and C. C. Tsai, *Phys. Rev. B* **32**, 32 (1985).
¹⁰M. Kumeda, A. Sugimoto, J. Zhang, Y. Ozawa, and T. Shimizu, *J. Non-Cryst. Solids* **164-166**, 1065 (1993).
¹¹J. Zhang, M. Kumeda, and T. Shimizu, *Jpn. J. Appl. Phys.* **33**, 1831 (1994).
¹²S. G. Bishop, U. Strom, and P. C. Taylor, *Phys. Rev. B* **15**, 2278 (1977).
¹³C. H. Seager and J. Kanicki, *Appl. Phys. Lett.* **57**, 1378 (1990).
¹⁴A. Morimoto, M. Matsumoto, M. Kumeda, and T. Shimizu, *Jpn. J. Appl. Phys.* **29**, L1747 (1990).
¹⁵S. Yamasaki, H. Okushi, A. Matsuda, and K. Tanaka, *Phys. Rev. Lett.* **65**, 756 (1990).
¹⁶W. Fuhs, in *Amorphous and Microcrystalline Semiconductor Devices, Materials and Device Physics*, edited by J. Kanicki (Artech House, Boston, 1992), p. 1.
¹⁷S. Yamasaki and J. Isoya, *J. Non-Cryst. Solids* **164-166**, 169 (1993).
¹⁸D. Adler, *Sol. Cell* **9**, 133 (1983).
¹⁹M. Nakata, S. Wagner, and T. M. Peterson, *J. Non-Cryst. Solids* **164-166**, 179 (1993).
²⁰E. Holzenkampfer, F.-W. Richter, J. Stuke, and U. Voget-Crote, *J. Non-Cryst. Solids* **32**, 327 (1979).
²¹J. C. Knight, R. A. Street, and G. Lucovsky, *J. Non-Cryst. Solids* **35-36**, 279 (1980).
²²H. Yokomichi, M. Kumeda, A. Morimoto, and T. Shimizu, *Jpn. J. Appl. Phys.* **24**, L569 (1985).